

# Prompt/Non-prompt $J/\psi$ production in proton-proton and Pb-Pb collisions with ALICE

Yuan Zhang on behalf of the ALICE Collaboration.

Email: e-mail: yuan.z@cern.ch

<sup>1</sup>State Key Laboratory of Particle Detection and Electronics,  
University of Science and Technology of China, Hefei 230026, China

**Abstract.** Quarkonium production in high-energy hadronic collisions is sensitive to both perturbative and non-perturbative aspects of QCD calculations. The charmonium production cross section can be split into prompt and non-prompt components, the first corresponding to a direct production of (anti-)charm quarks, the second originating from the decay of beauty hadrons. The latter is important to investigate the mass dependence of heavy-quarks in-medium energy-loss mechanism.

In this contribution the recent measurements of prompt and non-prompt  $J/\psi$  carried out by the ALICE Collaboration in pp and Pb–Pb collisions at midrapidity ( $|y| < 0.8$ ) will be presented. Moreover, thanks to the installation of the new muon forward tracker (MFT), the prompt/non-prompt charmonia separation is possible in LHC Run 3 also at forward rapidity ( $2.5 < y < 4$ ). The status of the new measurements will be presented.

## 1 Introduction

Charmonia, bound states of charm-anticharm pairs, are a robust system to test our understanding of quantum chromodynamics (QCD) [1, 2] and important probes to study the quark-gluon plasma (QGP), a state of strongly interacting matter where quarks and gluons are not anymore confined inside their hadronic bags. The QGP is expected to be produced at extremely high temperatures and energy densities, conditions that can be reproduced in the laboratory by colliding heavy ions at ultra-relativistic energies. While the production of the heavy-quark pair can be addressed with perturbative QCD, the bound state formation proceeds via a non-perturbative process and is subject to intense research [3].

In pp collisions at the LHC, the production of a heavy quark pair requires a large momentum transfer, which is still very small compared to the collision energy. Hence, multiple partonic interactions with momentum transfers similar to those required for heavy-quark production may occur in the same hadronic collision. Therefore, the measurement of heavy quarkonium as a function of charged hadron multiplicity contains information about the abundance of such multiple partonic interactions at these energy scales.

On the other hand, in Pb–Pb collisions at LHC energies, the production of  $J/\psi$  would be suppressed in the medium due to static colour screening resulting from the high density of colour charges inside the QGP [4] or due to dynamical dissociation [5]. However, at LHC energies, there is an additional contribution to the  $J/\psi$  production, known as regeneration,

according to which the abundantly produced charm and anti-charm quarks from different hard partonic scatterings can recombine to form charmonium states [6, 7].

Inclusive  $J/\psi$  production in high-energy hadronic collisions consists of several contributions: the  $J/\psi$  produced directly and from the decays of higher mass charmonium states, known as the "prompt" contribution, and  $J/\psi$  originating from the weak decays of beauty hadrons, referred to as "non-prompt". The measurement of prompt  $J/\psi$  production enables a direct comparison with prompt charmonium models. In addition, the non-prompt  $J/\psi$  production measurement provides a direct insight into the suppression of beauty hadrons.

## 2 Results of $J/\psi$ -hadron correlations in pp collisions

The measurement of associated hadron yields to  $J/\psi$  can provide more information to discriminate between different quarkonium production scenarios. In high-multiplicity events, it can shed more light on the underlying mechanisms leading to the increase of the  $J/\psi$  yields with multiplicity [8]. The correlation function  $C$  with electron-pairs and hadrons in a transverse momentum interval  $p_T^{J/\psi}$  and  $p_T^h$  respectively is calculated as:

$$C(\Delta\eta, \Delta\varphi; p_T^{J/\psi}, m_{e^+e^-}, p_T^h) = \frac{1}{N_{\text{trig}}} \cdot \frac{S(\Delta\eta, \Delta\varphi)}{B(\Delta\eta, \Delta\varphi)} \cdot B(0, 0) \quad (1)$$

where  $N_{\text{trig}}$  is the number of  $J/\psi$  triggers, while  $\Delta\eta$  and  $\Delta\varphi$  are the difference in pseudorapidity and azimuthal angle between the dielectron trigger and associated hadron. The  $S$  and  $B$  are the doubly-differential distributions of  $J/\psi$ -hadron pairs obtained from the same event or different events, respectively. The  $B(\Delta\eta, \Delta\varphi)$  from mixed-event is used to correct for geometrical acceptance effects and is normalized by  $B(0, 0)$ . The correlation function studied as a function of  $\Delta\varphi$  for several  $J/\psi$   $p_T$  and associated-hadron  $p_T$  intervals is fitted by:

$$C(\Delta\varphi) = b + a_{\text{NS}} \times e^{-\frac{(\Delta\varphi)^2}{2\sigma_{\text{NS}}^2}} + a_{\text{AS}} \times e^{-\frac{(\Delta\varphi - \pi)^2}{2\sigma_{\text{AS}}^2}}, \quad (2)$$

to get the contributions from the near-side (NS) and away-side (AS). And the baseline  $b$  is also determined from the fit of the correlation function with this formula.

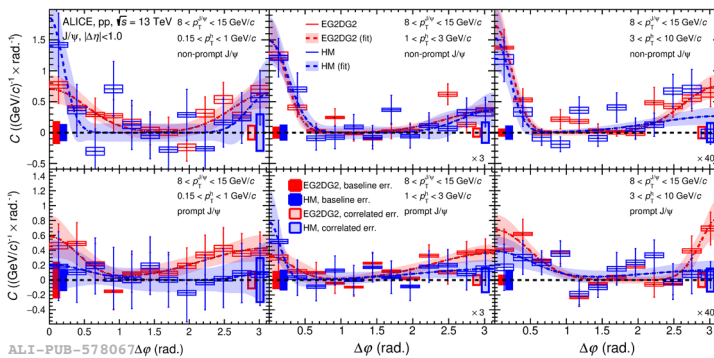


**Figure 1.** Baseline subtracted non-prompt (top panels) and prompt (bottom panels)  $J/\psi$ -hadron correlation functions with different triggers and associated hadrons in different  $p_T$  intervals [9]. The differential correlated yields are normalized per radiant and per  $\text{GeV}/c$ .

Figure 1 shows an example of a comparison of the baseline-subtracted correlation functions for non-prompt and prompt  $J/\psi$  in EG2DG2 (the sum of energy in a sliding window

of 4×4 towers in EMCAL above 4 GeV threshold) and HM (0.1% events with the highest multiplicity in the V0 detector) triggered events. Despite the significantly different baseline values ( $b$ ), due to the much higher multiplicity seen in the HM triggers, the two baseline-subtracted correlation functions show peak structures which are compatible within uncertainties for prompt and non-prompt J/ψ on both near and away sides.

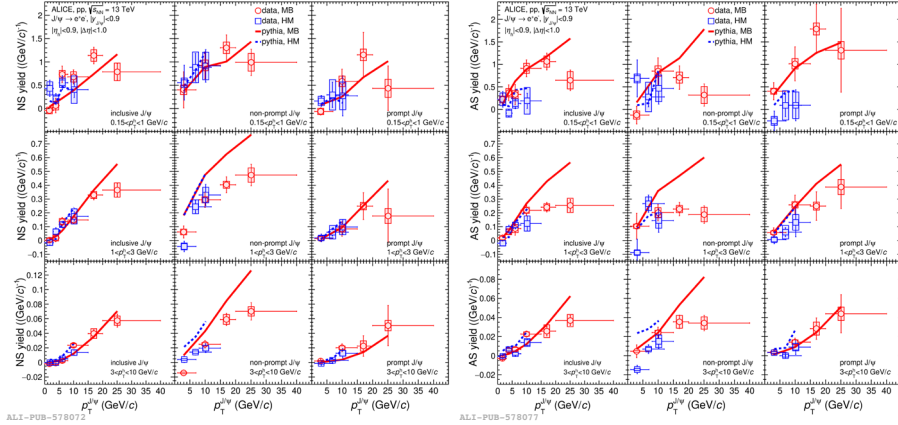


**Figure 2.** Near-side (left) and away-side (right) correlated particle yields as a function of the J/ψ trigger  $p_T$  for the inclusive, non-prompt, and prompt J/ψ and different associated  $p_T$  intervals [9]. Different color represent different triggers.

For a given  $p_T^h$  interval, the NS associated yields shown in Fig. 2 grow as a function of  $p_T^{J/\psi}$  for inclusive, prompt, and non-prompt J/ψ. The trend is significant for the hadrons with  $p_T^h > 1$  GeV/c, while for the lowest  $p_T$  the measurement precision does not allow to conclude. The near-side yields associated with non-prompt J/ψ are larger than those associated to prompt J/ψ. The associated yields observed in the HM triggered events and in MB (coincidence of signals in both V0 counters) triggered events show a good agreement within uncertainties for inclusive, non-prompt, and prompt J/ψ. This indicates that the parton fragmentation into J/ψ, prompt or non-prompt, is not significantly modified in events with high event activity relative to MB events. This is consistent with observations made in Ref. [10]. The PYTHIA calculations are generally in good agreement with NS results, however, hadron yields with  $p_T > 1$  GeV/c associated with non-prompt J/ψ are overestimated. This might point to hadronization effects which are not well reproduced in PYTHIA.

The away-side yields, related to the recoil jet, are shown in Fig. 2. The PYTHIA calculations are in good agreement with the results for prompt J/ψ over the entire  $p_T^{J/\psi}$  range, while for inclusive and non-prompt J/ψ, the model overestimates the measurements for  $p_T$  above 15 GeV/c. The associated yields obtained in HM triggered events are compatible with those obtained in MB/EMCAL triggered events. However, for prompt J/ψ and in the  $0.15 < p_T^h < 1.0$  GeV/c interval, there is a hint of lower correlated hadron yields in HM triggered events than in MB events. As also discussed in Ref. [11], the lower away-side yields are likely related to the definition of the HM trigger, which requires a high threshold on charged-particle multiplicity in the V0 detector acceptance. This introduces a bias towards events where the recoil jet is in the V0 acceptance, hence lower away-side yields would be seen at midrapidity.

### 3 Results of $J/\psi$ production in Pb–Pb collisions

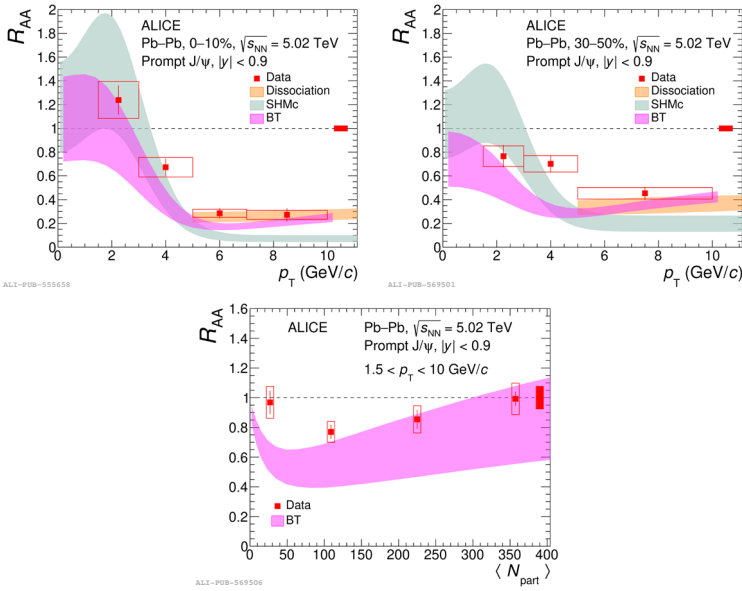


**Figure 3.** Prompt  $J/\psi$   $R_{AA}$  as a function of  $p_T$  and centrality in Pb–Pb collisions at  $\sqrt{s_{NN}} = 5.02$  TeV at midrapidity [12], compared with the model calculations from [13–17].

The prompt and non-prompt  $J/\psi$  nuclear modification factors ( $R_{AA}$ ) are measured at midrapidity using the dielectron channel [12]. Figure 3 presents the prompt  $J/\psi$  nuclear modification factor as a function of  $p_T$  and centrality compared with model calculations. The  $R_{AA}$  of prompt  $J/\psi$  is suppressed for  $p_T$  larger than 5 GeV/c and the suppression is stronger in central collisions. But for  $p_T$  less than 5 GeV/c, the  $R_{AA}$  is increasing towards low  $p_T$  which is likely driven by the regeneration process. The statistical hadronisation model (SHMc) [13] reproduces the prompt  $J/\psi$   $R_{AA}$  results at low  $p_T$ , while it is significantly below the data for  $p_T > 5$  GeV/c. The Boltzmann transport model (BT) [16, 17] provides a good description of the measurements in the full  $p_T$  range in 0–10% most central collisions, while the model underpredicts the data in peripheral collisions. The dissociation model [14], available only above 5 GeV/c, provides a good description of prompt  $J/\psi$   $R_{AA}$  measurements within uncertainties. The BT model, which shows a rising trend with increasing number of participants, is in good agreement with experimental results in central collisions. Below  $\langle N_{part} \rangle \sim 50$ , both the data and the model exhibit a similar increasing trend towards more peripheral collisions, however the agreement between data and model worsens.

The nuclear modification factor of non-prompt  $J/\psi$  is compared with models in Fig. 4. The LT1 [18] and POWLANG [21, 22] use the Langevin equation for describing the evolution of the beauty quarks through the QGP and an improved Langevin approach is used in the LT2 [19] model but only collisional processes are considered in POWLANG. The POWLANG model is also calculated with different transport coefficients obtained either from the hard thermal loop (HTL) or lattice QCD (LatQCD). An extended linear Boltzmann transport equation is used in the LBT [20] model. The CUJET3.1 [23, 24] framework is used to evaluate the jet energy loss in a hydrodynamic background. The DREENA-A [25, 26] model combines the dynamical energy loss model with hydrodynamical simulations. And

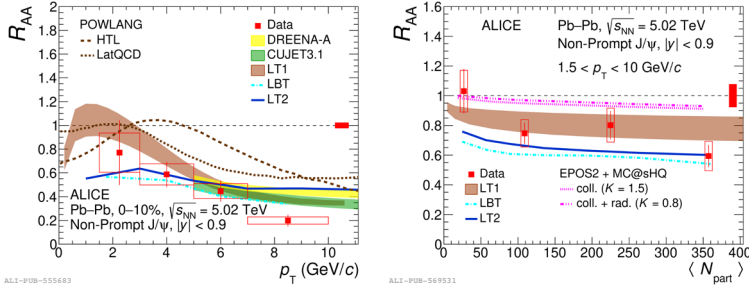


**Figure 4.** Non-prompt  $J/\psi$   $R_{AA}$  as a function of  $p_T$  and centrality in Pb–Pb collisions at  $\sqrt{s_{NN}} = 5.02$  TeV at midrapidity [12], compared with the model calculations from [18–27].

in the EPOS2+MC@sHQ [27] model, the initial conditions from EPOS2 is combined with the Monte Carlo treatment of the Boltzmann equation of heavy quarks, using cross sections rescaled by a global factor  $K$  and with or without including radiative processes. All available model predictions except POWLANG show compatible values for  $p_T$  above 5 GeV/c, and within uncertainties are in an overall good agreement with the data. The POWLANG model overpredicts the  $R_{AA}$  at high  $p_T$ , which might be a consequence of the lack of radiative energy loss contributions in this model. Below 5 GeV/c, the LT1 and POWLANG models sit on the upper side of the data points, still being compatible with them within uncertainties, while the EPOS2+MC@sHQ model overpredicts the measurements. Both LBT and LT2 models are compatible with the measured  $R_{AA}$  within uncertainties in the full measured  $p_T$  range. In the right plot, the LT1 model shows a slightly decreasing trend towards central collisions, and is compatible with data within uncertainties for all centrality classes. The LBT, LT2 and EPOS2+MC@sHQ models predict a similar decreasing trend towards larger  $\langle N_{part} \rangle$ . The LBT and LT2 models show good agreement with  $R_{AA}$  results in 0–10% centrality class, while for other centrality classes both models slightly underpredict the data. The EPOS2+MC@sHQ model agrees with data in the most peripheral class, while it tends to overestimate measurements towards more central collisions.

## 4 Measurement of prompt and non-prompt $J/\psi$ at forward rapidity

Thanks to the installation of the Muon Forward Tracker (MFT) detector in Run 3, the prompt and non-prompt  $J/\psi$  can be separated at forward rapidity by the pseudoproper decay length ( $l_{J/\psi}$ ) as shown in Fig. 5. The ability to distinguish prompt and non-prompt  $J/\psi$  at forward rapidity provides a powerful new tool to study the behavior of charm and beauty quarks in QGP.

## 5 Summary

In this contribution, recent measurements of  $J/\psi$ -hadron correlations in pp collisions and  $R_{AA}$  for prompt and non-prompt  $J/\psi$  are reported. In pp collisions, the near-side yields associated with non-prompt  $J/\psi$  are larger than those associated with prompt  $J/\psi$  and there is no strong multiplicity dependence observed in charm and beauty fragmentation. In Pb–Pb collisions, the  $R_{AA}$  of prompt  $J/\psi$  increases towards low  $p_T$  and most central collisions and can be described by models considering regeneration in low  $p_T$ . The models with energy loss in medium can describe the  $R_{AA}$  of non-prompt  $J/\psi$ . Thanks to the MFT detector, the prompt and non-prompt  $J/\psi$  can be separated at forward rapidity in Run 3.

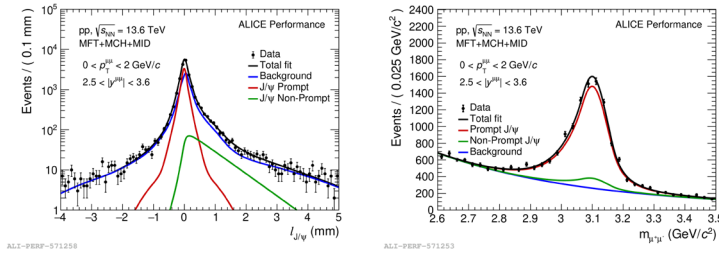


**Figure 5.** Separation of prompt and non-prompt  $J/\psi$  at forward rapidity in pp collisions in by the pseudo-proper decay length (left), and the signal extraction for prompt and non-prompt  $J/\psi$  (right).

## 6 Acknowledgement

The author is supported in part by the National Key R&D Program of China under Grant No. 2018YFE0104900, the National Natural Science Foundation of China under grant No. 12061141008 and 12105277.

## References

- [1] N. Brambilla et al., *Eur. Phys. J. C* **71** (2011) 1534.
- [2] ALICE Collaboration, S. Acharya et al., *Eur. Phys. J. C* **84** no. 8, (2024) 813.
- [3] Emilien Chapon et al., *Prog. Part. Nucl. Phys.* **122** (2022) 103906.
- [4] T. Matsui et al., *Phys. Lett. B* **178** (1986) 416–422.
- [5] Alexander Rothkopf et al., *Phys. Rept.* **858** (2020) 1–117.
- [6] P. Braun-Munzinger et al., *Phys. Lett. B* **490** (2000) 196–202.
- [7] Robert L. Thews et al., *Phys. Rev. C* **63** (Apr, 2001) 054905.
- [8] Jean-Philippe Lansberg et al., *Phys. Rept.* **889** (2020) 1–106.
- [9] ALICE Collaboration, Shreyasi Acharya et al., *JHEP* **07** (2025) 023.
- [10] ALICE Collaboration, Shreyasi Acharya et al., *Eur. Phys. J. C* **82** no. 4, (2022) 335.
- [11] ALICE Collaboration, Shreyasi Acharya et al., *JHEP* **05** (2024) 229.
- [12] ALICE Collaboration, Shreyasi Acharya et al., *JHEP* **02** (2024) 066.
- [13] Anton Andronic et al., *Phys. Lett. B* **797** (2019) 134836.
- [14] Samuel Aronson et al., *Phys. Lett. B* **778** (2018) 384–391.
- [15] Yiannis Makris et al., *JHEP* **10** (2019) 111.
- [16] Kai Zhou et al., *Phys. Rev. C* **89** no. 5, (2014) 054911.
- [17] Baoyi Chen et al., *Chin. Phys. C* **43** no. 12, (2019) 124101.
- [18] Meimei Yang et al., *Phys. Rev. C* **107** no. 5, (2023) 054917.
- [19] Shu-Qing Li et al., *Eur. Phys. J. C* **81** no. 11, (2021) 1035.
- [20] Wen-Jing Xing et al., *Phys. Lett. B* **838** (2023) 137733.
- [21] Andrea Beraudo et al., *JHEP* **05** (2021) 279.
- [22] A. Beraudo et al., *Eur. Phys. J. C* **75** no. 3, (2015) 121.
- [23] Shuzhe Shi et al., *Chin. Phys. C* **43** no. 4, (2019) 044101.
- [24] Shuzhe Shi et al., *Chin. Phys. C* **42** no. 10, (2018) 104104.
- [25] Dusan Zigic et al., *Front. in Phys.* **10** (2022) 957019.
- [26] Stefan Stojku et al., *Phys. Rev. C* **105** no. 2, (2022) L021901.
- [27] Marlene Nahrgang et al., *Phys. Rev. C* **93** no. 4, (2016) 044909.